An Efficient, Electrically Small Antenna Designed for VHF and UHF Applications

Richard W. Ziolkowski, *Fellow, IEEE*

***Abstract*—An electrically small electric-based metamaterial-inspired antenna that is designed for narrow bandwidth operations in the VHF and UHF bands is presented. It is demonstrated that the idealized lossless versions have overall efficiencies at 100% without any external matching circuits and quality factors approaching the Chu limit. When conductor losses are introduced, the overall efficiencies remain high.**

***Index Terms*—Antenna theory, electrically small antennas, metamaterials, parasitics, quality factors.**

I. Introduction

THE proliferation of wireless devices for communication and sensor applications has re-stimulated the need for efficient, broad bandwidth, easy-to-build and inexpensive electrically small antennas (ESAs). These often conflicting requirements have made the design tasks onerous for antenna engineers with traditional schemes. Typically, an electrically small radiator exhibits an input impedance that is characterized by a large reactance and a low radiation resistance. Traditionally then, to achieve an efficient radiator, one introduces an external matching circuit that provides the necessary complex conjugate reactance to achieve a total input reactance of zero and further introduces a quarter-wavelength resistance transformer to match the now resonant or anti-resonant radiating element to the source. A different paradigm, enabled by metamaterials, to achieve efficient ESAs without the need for these external matching circuits has been considered in [1]–[6].

The EZ antennas introduced in [4]–[6] employed metamaterial-inspired structures that are placed in the very near field of the bare radiator to achieve complete matching of the resulting antenna system to the source. These parasitic structures are not metamaterials themselves; but they are inspired by that possibility, i.e., when they are treated instead as a unit cell, the resulting metamaterial exhibits the ENG or MNG behavior needed to achieve the resonant interactions essential to the metamaterial-based antennas described in [1]–[3]. Lumped element versions of the metamaterial-inspired 2D magnetic EZ antennas have been tested experimentally; the agreement with the numerical predictions was very good [6]. The lumped element versions are important because they provide a direct path to realize tunable, low frequency antennas. They also allow for the possibility that active lumped elements, such as amplifiers, could be introduced to overcome losses and to increase the bandwidth. In this paper, encouraged by their successful use in [6], a corresponding lumped element electric antenna is introduced and is called the Z antenna because of its shape.

Manuscript received February 22, 2008. This work was supported in part by DARPA under Contract HR0011-05-C-0068.

The author is with the Department of Electrical and Computer Engineering, University of Arizona, Tucson, AZ 85721-0104 USA (e-mail: ziolkowski@ece.arizona.edu).

Color versions of one or more of the figures in this paper are available online at http://ieeexplore.ieee.org.

Digital Object Identifier 10.1109/LAWP.2008.921635

II. Metamaterial-Inspired Z Antenna Design

The Z antenna geometry is shown in Fig. 1 along with definitions of its dimensions. The Z antenna is a simplification of the 2D electric EZ antenna reported in [6]. The meanderline of that design has been reduced to the two split "J's" connected by the lumped element inductor that form the Z-shaped parasitic element. Instead of tuning the inductance to achieve complete matching by changing the length, thickness and height of the meanderline, the inductance value of the lumped element is tuned. Thus, the lumped element enables a large variation of the resonant frequency. The thickness of the copper has been enlarged greatly from the meanderline design to achieve smaller current densities and, hence, lower conductive losses. The dimensions for the 1000 nH, lossless case are explicitly: air gap $\mathrm{T1} = 0.787$mm, copper thickness $\mathrm{T2} = 1.7$ mm, inductor height $\mathrm{T3} = 1.52$ mm, LRC element location $\mathrm{T4} = \mathrm{T3}/2$, monopole thickness ($\sim$ 2 oz. copper) $\mathrm{T5} = 0.068$ mm, Z element length $\mathrm{L1} = 10$ mm, copper height $\mathrm{W1} = 2$ mm, copper width $\mathrm{W2} = 2$ mm, inductor length $\mathrm{L2} = 2.29$ mm, inductor width $\mathrm{W3} = 1.73$ mm, thickness of the inductor endcaps $\mathrm{L3} = 0.3$ mm, gap width $\mathrm{g} = 0.5$ mm, coax inner conductor radius a = half width of monopole $= 0.75$ mm, coax outer conductor radius $\mathrm{b} = 2.301a = 1.72575$ mm, and antenna height $\mathrm{H1} = 2.9$ mm. The inductor was modeled as a dielectric block with permittivity $\varepsilon_r = 2.2$ and with the HFSS LRC element (specifying only inductance values) centered and parallel to the faces of the Z structure.

Because of the very small physical sizes relative to the wavelength and because of the desire to investigate very narrow bandwidth behaviors, the simulations were challenging. They were run on a 64-bit platform with ANSOFT's HFSS v.10.2. The radiation boundary surfaces, as recommended by ANSOFT, were set slightly larger than $\lambda_{\mathrm{res}}/4$ away from the Z antenna. The minimum convergence parameter was set at $\Delta S = 1.0 \times 10^{-4}$ to achieve adequate mesh resolution to obtain the necessary frequency resolution of the responses. All of the conductor volumes were pre-meshed to improve convergence. The radiation boundary surface was also pre-meshed to obtain the most accurate overall efficiency values. The lumped element was modeled with the HFSS RLC element. The diameter of the center conductor of the coax matched the width of the monopole stub; the outer radius of the coax was set to 2.301

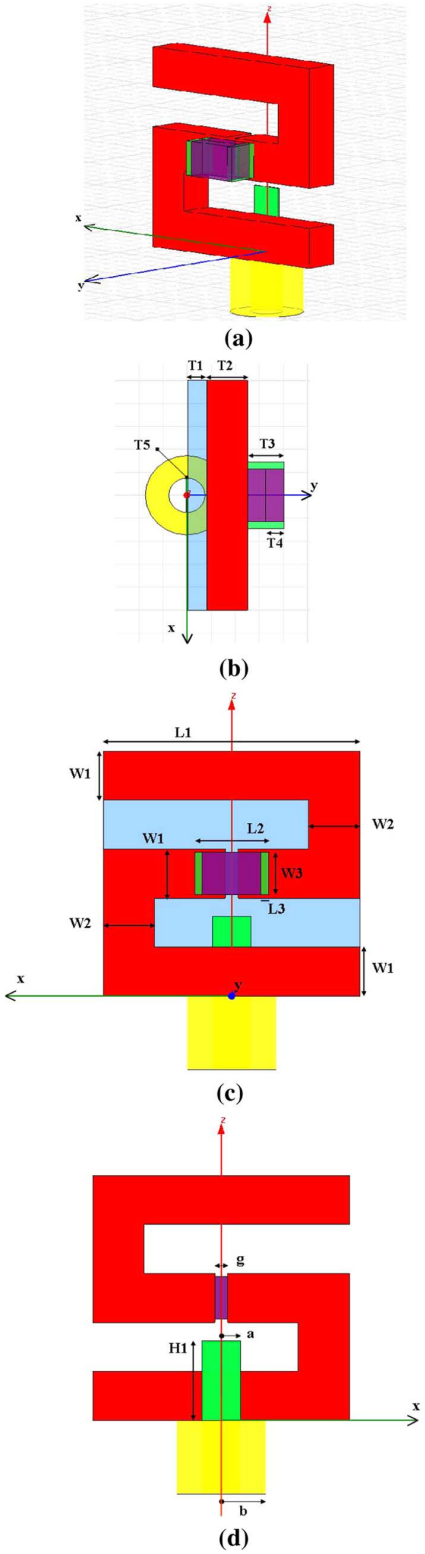

Fig. 1. The Z-antenna and its dimensions (a) 3D view, (b) top view, (c) inductor side view, and (d) monopole side view.

times the radius of the center conductor to achieve approximately a 50 Ω source impedance (e.g., the actual simulation value was 49.969 Ω for the 1000 nH case). The dimensions of the lumped element model were based on those of the API Delevan Series 0805 wire wound surface mount inductor [7]. For all of the lossless cases, an idealized copper was used with $\sigma_{\text{ideal}} = 5.8 \times 10^{17}$ Siemens/m, whereas real copper was used for the lossy cases with $\sigma_{\text{real}} = 5.8 \times 10^{7}$ Siemens/m. While its coil is copper, the actual electromagnetic properties of the support materials used in the lumped element inductor are not available. Circuit simulations could include the measured circuit losses of the inductor, but they would not provide a self-consistent value of the radiation efficiency of this three-dimensional antenna system. Consequently, the lumped element was modeled as an ideal inductor and only the copper losses in the radiating elements were included in the lossy case simulations.

For all of the different frequency designs reported below, the only changes made were in the inductor value and in the height of the monopole antenna, i.e., for a specific lumped element value, the height of the monopole H1 was adjusted to re-establish complete impedance matching. For instance, when copper losses were included in the 1000 nH case, matching was re-established with $\mathrm{H1} = 3.137$mm. The minimum S_{11} values achieved were all below -40 dB at the resonant frequency. The HFSS predicted S_{11} values for the lossless and lossy 1000 nH cases are shown, respectively, in Fig. 2(a) and (b). The input impedance for the lossy case is illustrated in Fig. 2(c). Complete matching with only the near field parasitic Z element was clearly achieved.

The tunability of the design over the frequencies of interest is demonstrated in Fig. 3. The HFSS predicted resonance frequencies are plotted versus the inductor values. The lowest inductor value considered was 34 nH, giving an HFSS predicted resonant frequency $f_{\text{res}} = 1015.19$ MHz, on the high side of the UHF band. The largest inductor value considered was 8000 nH, giving an HFSS predicted resonant frequency $f_{\text{res}} = 67.399334$ MHz, on the low side of the VHF band. It was found that the resonant frequency scales simply as

$$f_{\text{res}} = \frac{1}{2\pi}\sqrt{\frac{1}{L_{\text{eff}}C_{\text{eff}}}}. \tag{1}$$

To verify this behavior, it was assumed that the effective inductance of the antenna was equal (because of its large magnitude) to the lumped element value. The effective capacitance value was then obtained by choosing, arbitrarily, the HFSS predicted resonance frequency of the lossless $L = 300$ nH case, $f_{\text{res}} = 355.571887$ MHz. It was then used to calculate resonant frequencies for all of the other lossless cases. The HFSS simulations were performed in the neighborhood of this predicted frequency and then only the height of the monopole was adjusted to achieve complete matching. A comparison between the analytical results obtained with (1) and the corresponding HFSS predicted values is shown in Fig. 3. The importance of (1) in the HFSS simulations can not be overstated. Because of how narrow band the resonances are in frequency, if there was not an *a priori* knowledge of where to look, the computer simulation time needed to search for them would have been unrealistic.

In all cases, the radius of the smallest enclosing sphere was $a = 11.25$ mm. Then, for instance, one finds at the resonant frequency for the lossless 1000 nH case, $f_{\text{res}} = 193.677876$ MHz, that $ka \simeq 0.046$. It is recalled that if the power provided by the

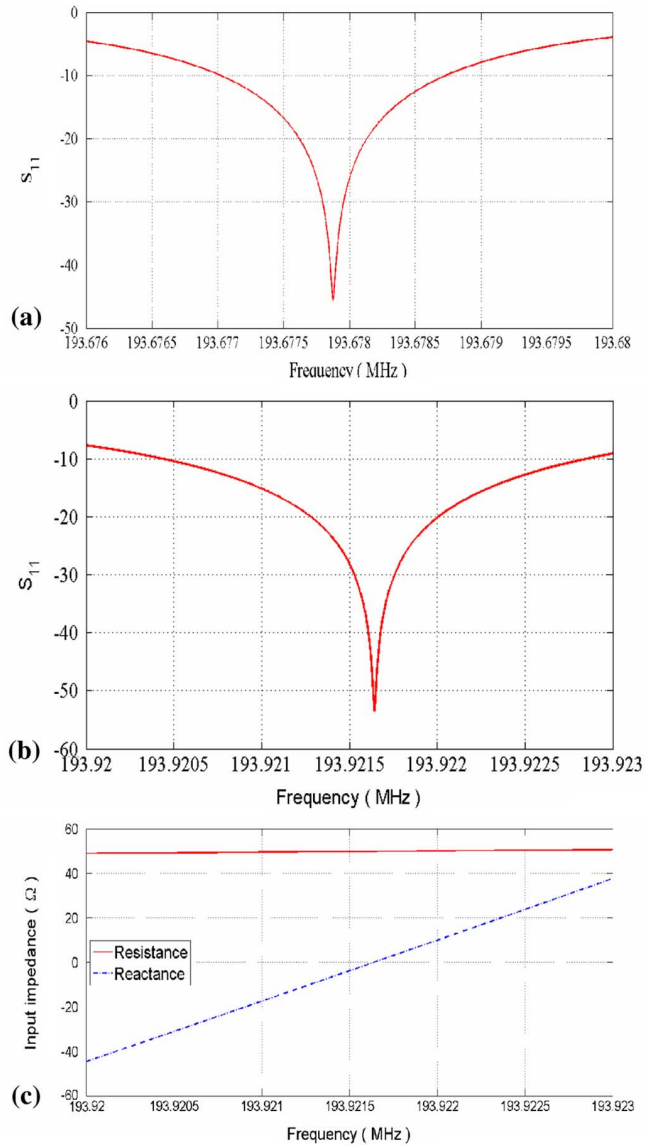

Fig. 2. HFSS-predicted values for the 1000 nH case. (a) S_{11} with no copper losses, (b) S_{11} with copper losses, and (c) input impedance with copper losses.

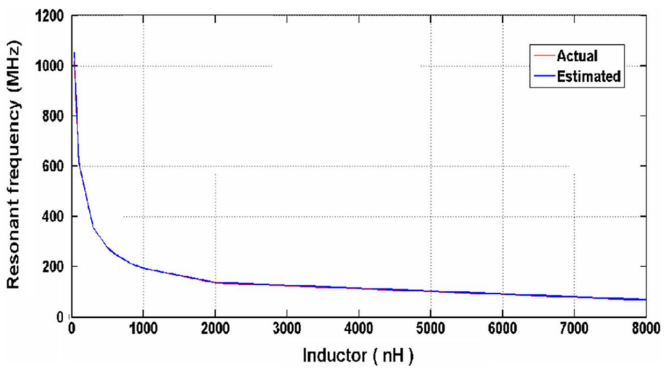

Fig. 3. Comparison of the analytical and HFSS-predicted resonant frequencies.

source is $P_{\rm in}$, the accepted power (AP), i.e., the power available at the terminals of the antenna, is $AP = (1 - |\Gamma|^2)\, P_{\rm in}$, where if $Z_{\rm ant} = R_{\rm ant} + j\, X_{\rm ant}$ is the input impedance of the antenna and Z_0 is the source impedance, the reflection coefficient

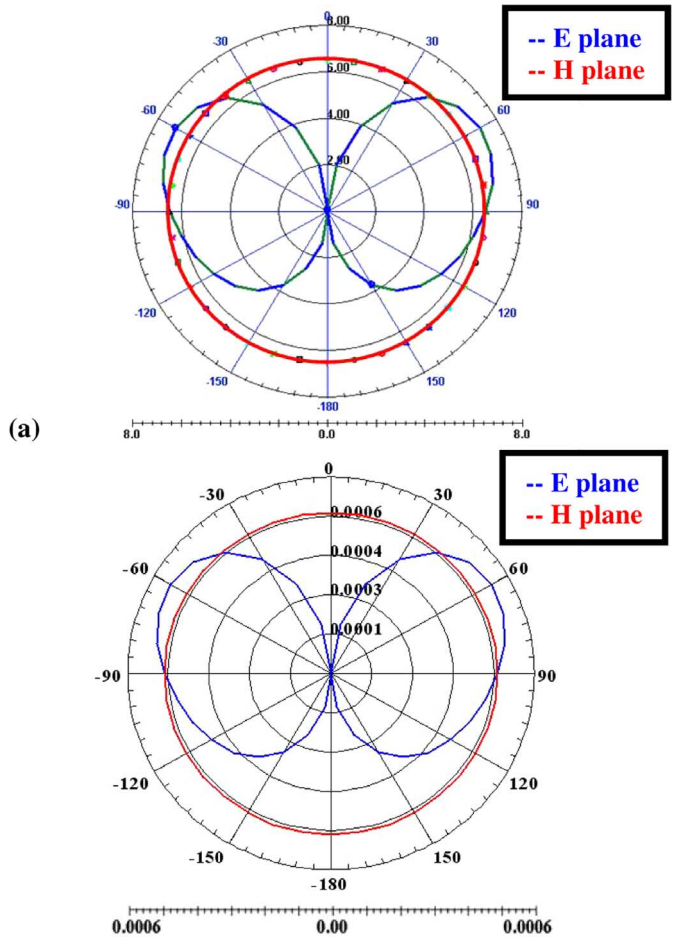

Fig. 4. E- and H-plane patterns for the lossless 1000 nH case (a) Z-antenna and (b) corresponding bare monopole.

$\Gamma = (Z_{\rm ant} - Z_0)/(Z_{\rm ant} + Z_0)$. Low S_{11} values, of course, correspond to high AP values. Furthermore, if the total power radiated is $P_{\rm rad}$, the radiation efficiency is $RE = P_{\rm rad}/AP$ and the overall efficiency is $OE = P_{\rm rad}/P_{\rm in}$. Because a very high degree of impedance matching was maintained, the accepted power was effectively 1 W for the 1 W source for all of the idealized lossless cases; and, subsequently, the overall efficiency was 100%. On the other hand, for the more realistic lossy 1000 nH case, the resonant frequency shifted to $f_{\rm res} = 193.921643$ MHz and the overall efficiency for this $ka \simeq 0.046$ ($\lambda_{\rm res}/a \simeq 137$) antenna was $OE = 71.19\%$. Several other lossy cases were also considered. For instance, with L = 100 nH, the resonance frequency was $f_{\rm res} = 610.78670$ MHz giving $ka \simeq 0.144$ ($\lambda_{\rm res}/a \simeq 44$) and the $OE = 93.42\%$. With L = 8000 nH, the resonance frequency was $f_{\rm res} = 67.688179$ MHz giving $ka \simeq 0.016$ ($\lambda_{\rm res}/a \simeq 394$) and the $OE = 34.39\%$, a still respectable value.

How do these results compare to the monopole itself, with no matching element? The HFSS-predicted far field E- and H-plane patterns produced by the lossless 1000 nH Z-antenna are shown in Fig. 4(a). The corresponding HFSS-predicted far field E- and H-plane patterns produced by the bare lossless coax-fed monopole (the same case with the Z element removed) are shown in Fig. 4(b). Because the Z-antenna is electrically small, the shapes of its patterns coincide with those of the

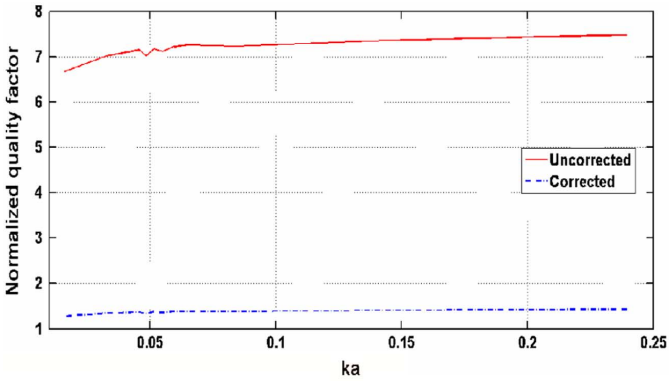

Fig. 5. HFSS-predicted Q values for the Z-antenna.

bare radiator. The impact of the finite ground plane is immediately apparent in the E-plane patterns. On the other hand, the amplitudes are notably different. This lossless $\mathrm{H1} = 2.9$ mm coax-fed monopole had an HFSS predicted input impedance of $Z_{\mathrm{in}} = 0.00238 - j\,7801.2$, which resulted in an accepted power $AP = 7.82 \times 10^{-9}\,W$. This confirms that the near field parasitic Z element does indeed act as an internal matching network for the overall antenna system and enables the resulting high overall efficiencies.

The main reason to even consider the idealized lossless cases is to provide the simplest calculation of the quality factors of these antennas. If losses were present, the radiation efficiency of each case would have to be calculated and included as indicated, for instance, in [8]. If $f_{\pm 3\mathrm{dB}}$ are the half- power frequency values, i.e., the -3 dB points of the S_{11} curves, then the VSWR fractional bandwidth is given by the well-known expression $FBW_{\mathrm{VSWR}} = (f_{+3\mathrm{dB}} - f_{-3\mathrm{dB}})/f_{\mathrm{res}}$ and the corresponding Q value can then be obtained as $Q_{\mathrm{VSWR}} = 2/FBW_{\mathrm{VSWR}}$ [9], without any adjustments for the radiation efficiency since its value is unity for all the lossless cases considered here. These Q_{VSWR} values for all the lossless cases are shown in Fig. 5 normalized to the Chu limit value [10]

$$Q_{\mathrm{Chu}} = \frac{1}{ka} + \frac{1}{(ka)^3} \tag{2}$$

For instance, for the 1000 nH case, $Q_{\mathrm{Chu}} = 1.0523 \times 10^4$ so that $Q_{\mathrm{VSWR}}/Q_{\mathrm{Chu}} = 7.16$. This normalized Q value was also calculated using the quality factor expression given in [9]: $Q_{\mathrm{YB}} = f_{\mathrm{res}}\,|\partial_f Z_{\mathrm{ant}}(f_{\mathrm{res}})|/2R_{\mathrm{ant}}$. With a midpoint rule applied to the HFSS predicted input impedance values, one obtains $Q_{\mathrm{YB}}/Q_{\mathrm{Chu}} = 7.14$, in very good agreement. However, as argued in [11], because the Z-antenna does not fill its radiansphere, the Chu value should be renormalized by the fraction of the volume used by the antenna. The ratio of the radian-hemisphere volume, $2\pi a^3/3$, to the smallest rectangular parallelpiped that encloses the Z-antenna equals 5.2. The corrected normalized Q values are also given in Fig. 5. For the 1000 nH case, one then has $Q_{\mathrm{VSWR}}/Q_{\mathrm{Chu,\,corrected}} = 1.38$. This indicates that the electrically small Z-antenna is making effective use of its volume. Note that for the 1000 nH case, the $\mathrm{FBW}_{\mathrm{VSWR}} = 0.0027\%$, which is an extremely small fractional bandwidth. This further emphasizes the advantage in the numerical simulations of knowing that the resonance frequency scales as (1).

III. Conclusion

The electrically small Z-antenna was introduced and its performance was characterized numerically. Near perfect impedance matching to the source was enabled by introducing a parasitic lumped inductor-based Z element into the very near field of a coax-fed monopole. The resonance of the Z-antenna was tuned from the low end of the VHF band to the high end of the UHF band by simply changing the inductor value and readjusting the length of the monopole. The quality factors indicated an effective use of the antenna volume. Fabrication and testing of the Z-antenna is in progress. One important issue that these experiments will address is how the lumped element itself should be modeled not as a circuit element, but as an electromagnetic object. Additionally, the bandwidths predicted for the lower frequency cases are very small and may not be useful for many practical applications. Approaches that could lead to an increase in the usable bandwidth of the Z-antenna are also under consideration. These investigations and their outcomes will be addressed in future reports.

References

[1] R. W. Ziolkowski and A. Erentok, "Metamaterial-based efficient electrically small antennas," *IEEE Trans. Antennas Propag.*, vol. 54, pp. 2113–2130, Jul. 2006.

[2] R. W. Ziolkowski and A. Erentok, "At and beyond the Chu limit: Passive and active broad bandwidth metamaterial-based efficient electrically small antennas," *IET Microw., Antennas Propag.*, vol. 1, pp. 116–128, Feb. 2007.

[3] A. Erentok and R. W. Ziolkowski, "A hybrid optimization method to analyze metamaterial-based electrically small antennas," *IEEE Trans. Antennas Propag.*, vol. 55, pp. 731–741, Mar. 2007.

[4] A. Erentok and R. W. Ziolkowski, "An efficient metamaterial-inspired electrically-small antenna," *Microw. Opt. Tech. Lett.*, vol. 49, no. 6, pp. 1287–1290, 2007.

[5] A. Erentok and R. W. Ziolkowski, "Two-dimensional efficient metamaterial-inspired electrically-small antenna," *Microw. Opt. Tech. Lett.*, vol. 49, no. 7, pp. 1669–1673, 2007.

[6] A. Erentok and R. W. Ziolkowski, "Metamaterial-inspired efficient electrically small antennas," *IEEE Trans. Antennas Propag.*, vol. 56, pp. 691–707, Mar. 2008.

[7] API Delevan, Series 0805 R Wirewound Surface Mount Inductor Data sheet p. 12 [Online]. Available: http://www.delevan.com, (08/09/2007)

[8] S. R. Best, "Low Q electrically small linear and elliptical polarized spherical dipole antennas," *IEEE Trans. Antennas Propag.*, vol. 53, pp. 1047–1053, Mar. 2005.

[9] A. D. Yaghjian and S. R. Best, "Impedance, bandwidth, and Q of antennas," *IEEE Trans. Antennas Propag.*, vol. 53, pp. 1298–1324, Apr. 2005.

[10] J. S. McLean, "A re-examination of the fundamental limits on the radiation Q of electrically small antennas," *IEEE Trans. Antennas Propag.*, vol. 44, pp. 672–676, May 1996.

[11] H. D. Foltz and J. S. McLean, "Limits on the radiation Q of electrically small antennas restricted to oblong bounding regions," in *Proc. IEEE Antennas and Propagation Society Int. Symp.*, Jul. 11–16, 1999, vol. 4, pp. 2702–2705.